대 한 조 선 학 회 논 문 집
제44권 제1호 2007년 2월

Journal of the Society of Naval Architects of Korea
Vol. 44, No. 1, pp. 32-39, February 2007

알루미늄 판의 용접변형해석

이주성[†*], Nguyen Tan Hoi[*]

울산대학교 조선해양공학부[*]

Analysis of Weld-induced Deformation in Aluminum Plates

Joo-Sung Lee[†*] and Nguyen Tan Hoi[*]

School of Naval Architecture & Ocean Engineering, Univ. of Ulsan[*]

Abstract

A three-dimensional finite element model has been developed to simulate the MIG P/S welding process of two aluminum plates. The finite element calculations are performed using ANSYS finite element code, which takes into account the thermal and mechanical non-linear material properties. The results of finite element analysis compared with those of experiment to show its validity in view of distortions. Parametric studies are carried out on the validated model to assess the effects of various factors on the final residual distortion. Large deformations, temperature dependent material properties are included in the model. Finally, the formulas of fitting curves of angular distortion transverse shrinkage, and longitudinal shrinkage have been proposed.

※Keywords: Aluminum plate(알루미늄 판), Thermal elasto-plastic analysis(열탄소성해석), Weld-induced deformation(용접변형), Residual stress(잔류응력)

1. INTRODUCTION

In fusion welding, a weldment is locally heated by the welding heat source. Due to the non-uniform temperature distribution during the thermal cycle, incompatible strains lead to stresses. These incompatible strains due to dimensional changes associated with solidification of the weld metal, metallurgical transformation, and plastic deformation, are the sources of residual stresses and distortions. When welding processes and parameters are changed, the heat flow patterns are also changed. The change of heat flow pattern causes a change in the

접수일: 2006년 9월 4일, 승인일: 2006년 12월 18일
†교신저자, jslee2@mail.ulsan.ac.kr, 052-259-2162

distribution of incompatible strains, and this causes changes in shrinkage and distortion (Masubuchi 1980).

Welding-induced residual stresses and distortions can play a very important role in the reliable design of welded joints and welded structures(Lee 2004). These drawbacks are especially evident in thin plate and shell structures and have therefore inhibited progress towards lighter welded fabrication. (Mollicone et al. 2006, Song et al. 2004). However, the welding process itself is a very complex phenomenon, which has not been fully understood, so that the distribution and magnitude of residual distortions and residual stresses is not readily available from the literature.

Many researchers such as Michaleris and DeBiccari(1997), Teng et al.(2001), Li et al.(2004), Kim(2004, 2006) and Kim et al.(2006) showed that the transient temperature fields can be computed adequately using finite element methods, given some generic welding trials. The final elastic deformations of the structure, due to the accumulation of individual welds, can also be computed relatively easily, provided that the results from a thermal elasto-plastic stage are available. The challenge, therefore, is to simplify the intractable thermal elasto-plastic stage of the process, starting from a transient temperature field input and leading to outputs of angular deformation and contraction stress field (Mollicone et al. 2006).

In this paper, a 3-dimensional model is used to investigate the weld-induced distortion and temperature distribution of aluminum plate. The model is validated by comparing its results with those of experiment. Parametric studies are carried out on to derive the formulae of predicting weld-induced deformation.

2. MODELING FOR NUMERICAL ANALYSIS

As it can be seen in many literature, weld-induced deformation should be analyzed as the results of moving heat source on the finite body, for which heat source should be imposed on the finite area rather than a point. Fig. 1(a) shows the coordinate system. For the sake of symmetric situation in the geometric shape, boundary and loading condition, one half of the base plates can be modeled into finite element as in Fig. 1(b). Symmetric boundary conditions are imposed at nodes along x axis.

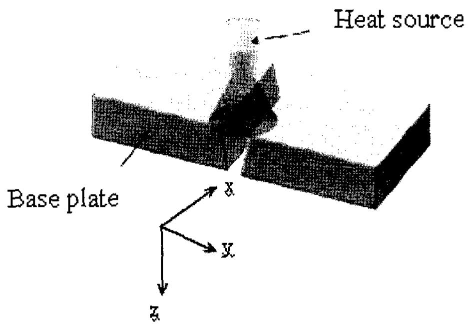

(a) definition of coordinate system

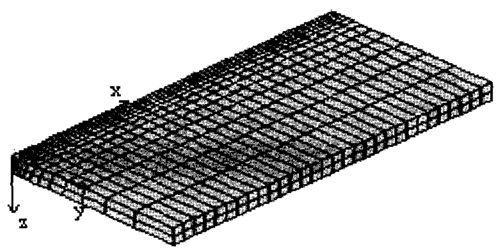

(b) finite element model of a half plate

Fig. 1 Coordinates and finite element modeling

Table 1 Welding conditions

Pass	Current (A)/ Voltage(V)	Φ (mm)	Speed (mm/s)	Root gap (mm)
1	19/130	3.0	7.0	3.2
2	19/140	3.0	7.0	

A 3-dimensional finite element model of a rectangular butt-joint weld in an aluminum plate with dimension L×B = 600mm × 150mm, thickness 6mm, groove angle 40° was tested with the welding conditions as shown in Table 1. It is assumed that only convective heat transfer occurs on the surface of the specimen and conductive heat transfer occurs within the specimen. Convection describes the effect of temperature gradients between the post-weld plate surfaces and the room temperature of the surrounding air that assumed to be 30oC. In this case, it has been assumed that the plate surface's temperature changes due to the combined effects of two conditions, namely, 1) conduction within the specimen, and 2) convection and emission from the specimen surface's temperature to the surrounding air temperature. The temperature within the specimen changes from weld pool to the location away from the weld pool due to heat conduction

The heat energy input to the weldment is generally calculated from the energy supplied. The heat input distribution will determine size and shape of the weld pool. In order to simulate the heat distribution and flow in the welding direction, the heat source is modelled as a three-dimensional moving heat source. The model of the heat source assumes a Gaussian heat flux distribution on the weld pool simulated by a cone. This model has capacity to be changed by the simple change of various geometrical parameter in order to simulate different weld pools that correspond to different welding parameters(Tsirkas et al. 2003).

In this study, the moving heat load of distributed heat flux is applied on the top surface of the model. The region on which heat is applied has a circular shape since the heat flux is appled perpendicularly to the plate without any inclination. The heat flux at a certain time and location within the surface of elements upon which the load is applied can be expressed as: (Fanous et al. 2003).

$$q(r)= \frac{3Q}{\pi r_b^2} e^{-3(r/r_b)^2} \quad (1)$$

The total heat input $Q=\eta VI$ is to be applied within the circle with radius r_b, where V and I are welding voltage and currency, respectively, and η is arc efficiency. $\eta = 0.75$ is given for the present study. 'r' illustrated in Fig. 2 denotes the distance from the center point of the heat source to the location at which the heat flux is applied. Therefore, it can be expressed by following Eq.(2).

$$r = \sqrt{(x-x_h)^2 + y^2} \quad (2)$$

$$\text{where } x_h = (t-t_0)v \quad (3)$$

Time t_0 is introduced since the center of the heat load approaches the first node of welding line apart from r_b. When the value of r is less than or equal to r_b, the heat flux is calculated from Eq.(1). Otherwise, the heat load is set to zero. r_b is assumed to be 5 mm in this study.

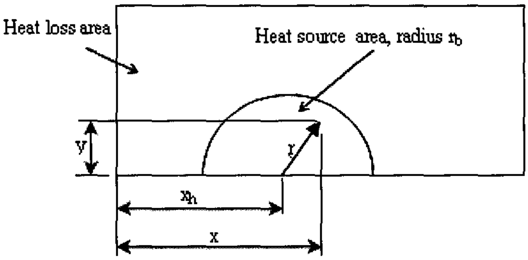

Fig. 2 Zones of heat flux and heat loss

The heat lost is calculated by Eq.(4) :

$$q = h_{convection}(T_i - T_a) + \epsilon_{em}\sigma_{bol}(T_i^4 - T_a^4) \quad (4)$$

The heat convection coefficient is 6W/m2.oC, which is assumed to be primarily dependent on the ambient temperature. The emissivity of radiative heat transfer is assumed to be 0.5. The temperature dependent physical and mechanical properties of AL5083 are shown as in Fig. 3.

3. NUMERICAL RESULTS AND DISCUSSIONS

In order to show the validity of the present numerical modeling, an experimental model which was conducted by Im et al.(2005) is selected. In the reference they used MIG P/S welding for aluminum alloy AL5083 with weldment material ER5183. The heat is generated by the discharge between the anode and the cathode using a consumable electrode.

The temperature histories obtained by finite element analysis are plotted at several z-positions along the line of x = 0 and at several y-positions along the line of z = 0. as shown in Fig. 4(a) and 4(b), respectively.

It can be seen that the temperature distribution decreases from top surface to bottom surface at z = 0 due to the gradient temperature from top to bottom surface. Fig. 5 shows the final deformed shape. It can be seen that deformation along the welding direction is nearly uniform.

The numerical results are compared in terms of vertical deflection along y direction as shown in Fig. 6. From this finding it can be said that the numerical results show good agreement with the experimental data.

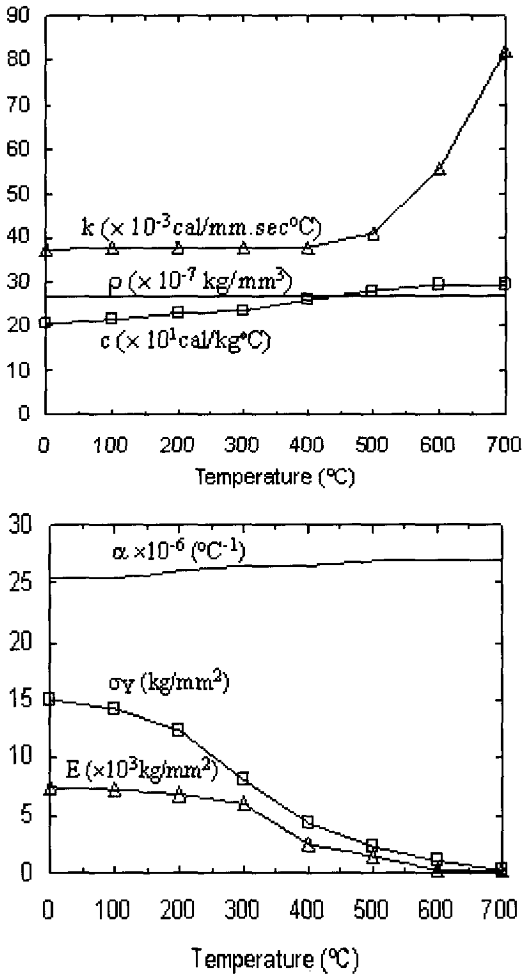

Fig. 3 Temperature dependent physical and mechanical properties of AL5083 (Im et al., 2005)

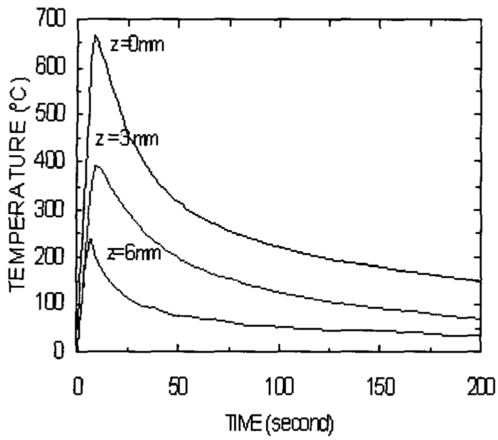

(a) several z-positions at x=0

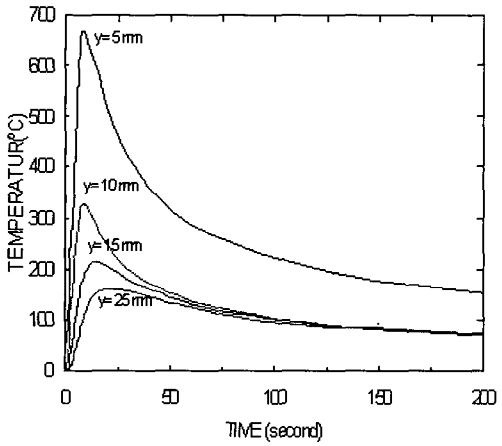

(b) several y-positions at z=0

Fig. 4 Transient temperature distribution

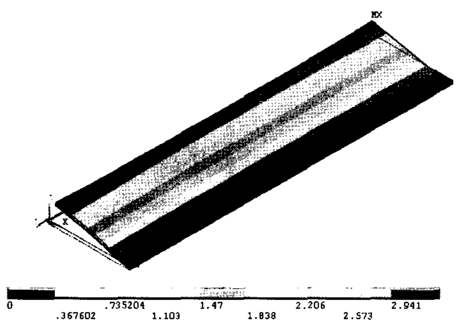

Fig. 5 Final deformed shape

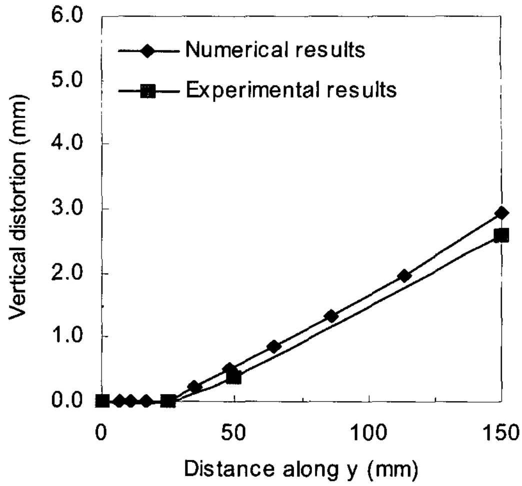

Fig. 6 Comparison of vertical distortion along y axis

4. FORMULAE OF PREDICTING WELD-INDUCED DEFORMATION

To derive some formulae of predicting weld-induced deformation, several parametric studies have been carried out with varying plate thickness and weld conditions. Models for the present parametric studies are listed in Table 2. As the present results, transverse shrinkage, longitudinal shrinkage and transverse angular distortion are plotted against the heat input parameter, q, in Figs. 7 to 9. Heat input parameter is, herein, defined as:

$$q = Q/t^2 \qquad (5)$$

where Q and t are heat input in J/mm and plate thickness in mm.

From Fig. 7 the linear relation between transverse shrinkage and heat input parameter is obtained. That means as the heat input parameter increases, the transverse shrinkage increases. The relation between longitudinal shrinkage is plotted in Fig. 8. Therefore the

Table 2 Models for parametric studies

Model	t (mm)	Welding condition			Heat input param-eter, q
		Ampere (A)	Voltage (V)	Speed (mm/s)	
AL-1	4	180	22	14.5	11.130
AL-2	4	180	22	15.0	10.759
AL-3	4	180	22	15.5	10.412
AL-4	5	190	22	13.5	8.076
AL-5	5	190	22	14.0	7.788
AL-6	5	190	22	14.5	7.519
AL-7	6	200	23	13.5	6.172
AL-8	6	200	23	14.0	5.952
AL-9	6	200	23	14.5	5.746
AL-10	7	220	23	13.0	5.180
AL-11	7	220	23	13.5	4.988
AL-12	7	220	23	14.0	4.810
AL-13	8	240	23	12.5	4.499
AL-14	8	240	23	13.0	4.326
AL-15	8	240	23	14.0	4.017
AL-16	9	250	23	12.0	3.857
AL-17	9	250	23	12.5	3.703
AL-18	9	250	23	13.0	3.561

Table 3 Mean and COV of formulae

Function	Mean	COV(%)
S_T/t	1.003	4.24
S_L/t	0.997	7.47
ϕ_T	0.988	19.10

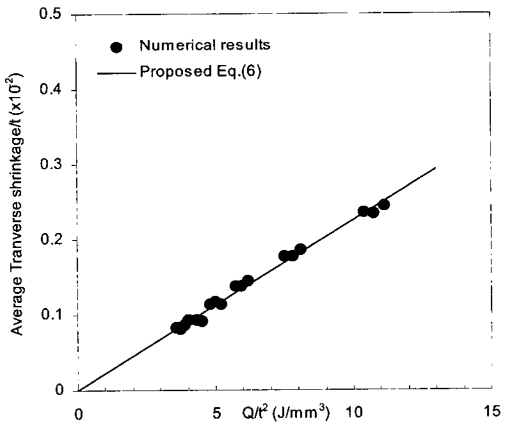

Fig. 7 Distribution of average transverse shrinkage S_T/t vs heat input parameter, q

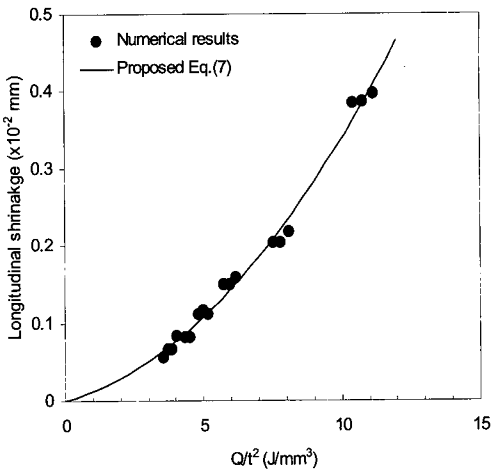

Fig. 8 Distribution of average longitudinal shrinkage S_L/t vs heat parameter, q

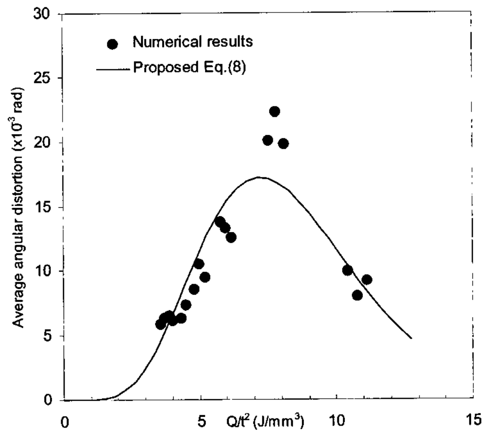

Fig. 9 Distribution of average angular distortion vs heat input parameter, q

longitudinal shrinkage will increase more than transverse shrinkage at the same heat input parameter.

In the case of angular distortion, the relation is an exponential equation which the angular distortion increases from 0 to about 17.0E-3 rad at heat input parameter 7.0 J/mm^3 and then decreases as shown in Fig. 9.

From the regression analysis formulae for transverse shrinkage, longitudinal shrinkage and transverse angular distortion are derived as following equations.

- for transverse shrinkage

$$S_T / t = 0.0226q \quad (6)$$

- for longitudinal shrinkage

$$S_L / t = \left(0.922q + 0.246q^2\right) \times 10^{-2} \quad (7)$$

- for transverse angular distortion

$$\phi_T = 0.0263q^{6.64} \exp(-0.92q) \quad (8)$$

where q is heat input parameter defined as Eq.(5).

Solid lines in Figs. 7 to 9 show the derived formulae. The mean and COV (coefficient of variation) of ratio between numerical results and equation (6), (7) and (8) are summarized in the Table 3. These equations well fit the numerical results such that their mean values are close to unity.

5. CONCLUSIONS

Based on the results from the benchmark analyses and parametric study, the simplified modeling process for simulating welding distortion using a general purpose FE package described here is reliable and instructive. The results are well agreed with the experimental data. Based on the parametric studies formulae for transverse shrinkage, longitudinal shrinkage and transverse angular distortion are derived, which would be useful in simply predicting the weld-induced deformation.

ACKNOWLEDGEMENT

This work was carried out with the supported by the University of Ulsan, Korea. The authors appreciate for the financial support of the University of Ulsan.

REFERENCES

- Fanous, I.F.Z., Younan, M.Y.A., and Wifi, A.S., 2003, "3-D Finite Element Modeling of the Welding Process Using Element Birth and Element Movement Techniques," Journal of ASME, Vol. 125, pp. 144-150.
- Im, D.Y, Kim, N.I, Lee, J.S., Lee, H.W and Choi, W.H, 2005. "A Study on Weldability and Strength of 5000 Aluminium Alloy," Proc. Welding Strength Committee Symposium, Korean Welding Society.
- Kim, J.T., Ha, Y.S. and Jang, C.D., 2006, "Analysis of Post Weld Deformation at HAZ by External Forces Based on Inherent Strain," Journal of Society of Naval Architecture of Korea, Vol. 43, No. 2, pp. 220-227.
- Kim, S.I., 2004, "Development of Simple Prediction Model for V-groove Butt Welding Deformation," Journal of Society of Naval Architecture of Korea, Vol. 41, No. 2, pp. 106-113.
- Kim, S.I., 2006, "Control of Welding Distortion for Thin Panel Block Structure Using Mechanical Tensioning Method," Journal of Society of Naval Architecture of Korea, Vol. 43, No. 1, pp. 68-74.
- Lee, J.S., 2004, "Simulator for Weld-Induced Deformation of Panel Blocks," Journal of Society of Naval Architecture of Korea, Vol. 41, No. 1, pp. 55-63.
- Li, Y., Wang, J., Chen, M. and Shen, X, 2004, "Finite Element Analysis of Residual Stress in the Welded Zone of a High Strength Steel," Bulletine of Material Science, Vol. 27, No. 2, pp. 127-132, Indian Academy of Science.

- Masubuchi, K., 1980, Analysis of Welded Structure, Pergamon Press, Oxford.
- Michaleris, P. and DeBiccari, A., 1997, "Prediction of Welding Distortion," Welding Journal, Vol. 76, No. 4, pp. 172s-180s.
- Mollicone, P., Camilleri, D., Gray, T.G.F. and Comlekci, T., 2006, "Simple Thermo-Elastic-Plastic Models for Welding Distortion Simulation," Journal of Materials Processing, Vol. 176, Issues 1-3, pp. 77-86.
- Song, H.C., Jo, Y.C. and Jang, C.D., 2004, "Numerical Analysis and Experimental Verification of Relaxation and Redistribution of Welding Residual Stresses," Journal of Society of Naval Architecture of Korea, Vol. 41, No. 6, pp. 84-90.
- Teng, T.L., Fung, C.P., Chang, P.H. and Yang, W.C., 2001, "Analysis of Residual Stresses and Distortions in T-joint Fillet Welds," Journal of ASME, Vol. 78, pp. 523-538.
- Tsirkas, S.A., Papanikos, P. and Kermanidis, T., 2003, "Numerical Simulation of the Laser Welding Process in Butt-Joint Specimens," Journal of Materials Processing Technology, Vol. 134, pp. 59-69.

< 이 주 성 >

< Nguyen Tan Hoi >